Peer-reviewed version available at Nanomaterials 2018, 8, 946; doi:10.3390/nano8110946

Article

Green synthesis of Ag nanoparticles using grape stalk waste extract for the modification of screen-printed electrodes

Julio Bastos-Arrieta[1,2]*, Antonio Florido[1,3], Clara Pérez-Ràfols[4], Núria Serrano[4], Núria Fiol[5], Jordi Poch[6], Isabel Villaescusa[5]

[1]Departament d'Enginyeria Química, Escola d'Enginyeria de Barcelona Est (EEBE), Universitat Politècnica de Catalunya. BarcelonaTEch (UPC), Av. Eduard Maristany, 10-14, 08019 Barcelona, Spain

[2]Physical Chemistry TU Dresden, Zellescher Weg 19, 01062 Dresden, Germany

[3]Barcelona Research Center for Multiscale Science and Engineering, Av. Eduard Maristany, 10-14, 08019 Barcelona, Spain

[4]Departament d'Enginyeria Química i Química Analítica, Facultat de Química, Universitat de Barcelona, c/ Martí i Franquès 1-11, 08028 Barcelona, Spain

[5]Departament d'Enginyeria Química, Escola Politècnica Superior, Universitat de Girona, c/ Mª Aurèlia Capmany, 61, 17071 Girona, Spain

[6]Departament d'Informàtica Aplicada i Matemàtiques, Escola Politècnica Superior, Universitat de Girona, c/ Mª Aurèlia Capmany, 61, 17071 Girona, Spain

*Corresponding Author: Dr. Julio Bastos-Arrieta: julio.bastos@tu-dresden.de and Dr. Nüria Fiol nuria.fiol@udg.edu

Abstract: The chemical synthesis of silver nanoparticles (Ag-NPs) by using an environmentally friendly methodology for their preparation is presented. Thus, considering that plants possess components that can act as reducing agents and stabilizers in the nanoparticles production, in this work, the synthesis of Ag-NPs by using a solution of grape waste extract as reducing and capping agent is studied. First, the total polyphenols content and reducing sugars in extracts produced at different conditions are characterized. After that, Ag-NPs are synthesized regarding the interaction of Ag ions (from silver nitrate) and the grape waste extract. The effect of temperature, contact time, extract/metal solution volume ratio and pH solution in the synthesis of metal nanoparticles are studied too. Different sets of nanoparticle samples are fully characterized by means of Electron Microscopy coupled with Energy Dispersive X-Ray for qualitative chemical identification. Ag-NPs with an average diameter of 27.7 ± 0.6 nm are selected to proof their suitability for sensing purposes. Thus, screen-printed electrodes modified with Ag-NPs are tested for the simultaneous voltammetric stripping determination of Pb(II) and Cd(II). Results indicate good reproducibility, sensitivity and limits of detection around 2.7 μg L^{-1} for both metal ions.

Keywords: silver nanoparticles, screen printed electrodes, grape stalk, green synthesis, voltammetry, metal analysis

Peer-reviewed version available at Nanomaterials 2018, 8, 946; doi:10.3390/nano8110946

1. Introduction

Several recent publications review the greener routes to metal nanoparticles synthesis mediated by microorganisms [1], algae and waste material [2], and plant materials extract [3,4]. The different routes to synthetize silver nanoparticles (Ag-NPs) have also been reviewed recently [5]. Some authors underline the advantages of using plant derivatives extracts over microorganisms. Plant derivatives extract has no need of neither cells culture maintenance nor sterile conditions [6,7]. Moreover, plant extracts provide natural capping agents for the stabilization of nanoparticles, therefore reducing the nanoparticles synthesis process to a single step [8]. All these advantageous features of plant extract result in a less reagent consumption and, consequently, in a reduction of the cost that facilitates the development of large scale production of nanoparticles in an environmental friendly approach. The synthesis of silver nanoparticles mediated by plant extract, recently reviewed by Ahmed [8] and Kuppusamy [9], reveals that reduction and stabilization of the nanoparticles is performed by combination of different biomolecules such as proteins, amino acids, enzymes, polysaccharides, alkaloids, tannins, phenolic acid, terpenoids and flavonoids. The content of these biomolecules acting as reducing and capping agents is known to be dependent on the source of the extract, providing different characteristics (i.e size, shape, stability) to the synthetized nanoparticles. In spite of the importance of the extract composition on the reduction process, few researchers reporting nanoparticles biosynthesis provide information about the main reducing components of the extract.

Grape stalks (GS) are the lignocellulosic skeleton of grape and account for the main by-product after grape harvesting and wine production. The extract of some grape sub-products such as leaves, stems, seeds and dried fruit, has been used for the production of bimetallic Fe/Pd [10], Fe_3O_4-Ag [11] and silver [12] nanoparticles, respectively. Three different grape wastes (seed, skin and stalk) were used by Krishnaswamy *et al*. [13], for the production of gold nanoparticles. A chemical characterization of grape stalk carried out recently [14] revealed that the main components of this by-product are polar compounds soluble in hot water with a high content in tannins and other polyphenolic compounds.

Nanoparticles (NPs) have been widely applied in different research fields due to their surface-volume ratio that provides them unique and improved properties in comparison to the analogous bulk material. One interesting feature of NPs (e.g. Ag-NPs) is the ease of their application in the modification of screen-printed electrodes (SPEs), which nowadays are a great platform for environmental portable electroanalysis due to their commercial availability, relatively low cost and reproducibility. Nanoparticles enhance the electron transfer among redox centers between the analyte and the electrode, reducing the over potentials of several analytically important electrochemical reactions [15,16]. Although the use of NPs have already been successfully applied to the development of new electrochemical sensors for the determination of heavy metal ions[17,18], to the best of our knowledge no previous research about the implementation of green-synthetized NPs has been published.

Here we report the synthesis of silver nanoparticles (Ag-NPs) mediated by the use of the aqueous extract of grape stalk waste with the evaluation of different factors that affect the synthesis of these NPs. Moreover, and for first time, the feasibility of these green synthesized Ag-NPs for electrochemical assays is presented. For this purpose, screen-printed carbon nanofibers electrodes (SPCNFE), which has been demonstrated to be a very suitable support for the modification of sensors[19], are modified with Ag-NPs using the drop casting approach and the resulting modified sensor is applied to the simultaneous determination of Cd(II) and Pb(II) ions in aqueous solution as a model metal ion system.

2. Materials and Methods

2.1 Reagents and materials

Grape stalk waste from wine production was kindly supplied by a winemaking cooperative (Empordà-Costa Brava, Spain). The waste was rinsed abundantly with water, dried and cut to separate the pedicels from the stalk branches. The pedicels were then ground and sieved to get the desired particle size (1-1.6 mm).

Peer-reviewed version available at Nanomaterials 2018, 8, 946; doi:10.3390/nano8110946

10^{-2} mol L^{-1} Cd(II) and Pb(II) stock solutions were prepared from $Pb(NO_3)_2 \cdot 4H_2O$ and $Cd(NO_3)_2 \cdot 4H_2O$ respectively and standardized complexometrically [20]. 0.1 mol L^{-1} acetate buffer solution (pH 4.5) was used for pH control. Ultrapure water (Milli-Q plus 185 system, Millipore) was used in all experiments.

2.2 Preparation of grape stalks extract

The extract was obtained by placing grape stalks in a 200 mL round bottom flask and adding 100 mL of Milli-Q water. A reflux condenser was placed at the top of the flask. The device was placed in a heating mantle. Extracts were obtained at different temperatures (60-100ºC) and contact times (15-120 min). After this, the extract was separated from the solid by filtration using a cellulose paper and centrifuged 30 minutes at 5000 rpm (Universal 320, Selecta). Extract samples were analyzed in order to determine their content in total polyphenols and reducing sugars. Prior to the analysis, the loss of volume of the filtrate due to possible water evaporation was compensated by adding water to a total volume of 100 mL.

2.2.1 Determination of total phenolic and reducing sugars

The total polyphenol content of the filtrates was analyzed by the Folin-Ciocalteu method and the reducing sugars content was determined by reaction of the sample with Fehling's solution followed by iodimetric titration of the unreduced copper remaining in the solution. A statistical analysis of experimental data (total polyphenols and reducing sugars) was performed to determine which of the studied parameters (temperature and extraction time) had a significant influence on the concentration of total polyphenols and reducing sugars of the obtained extracts. This statistical analysis was performed using SPSS software program for Windows with a significance level of 0.05 (confidence interval 95%).

2.3 Synthesis of silver nanoparticles

2.3.1 General procedure of synthesis using grape stalk as reducing agent

Synthesis of silver nanoparticles was carried out by putting into contact a certain volume of extract with a certain volume of 0.01 mol L^{-1} silver nitrate solution in sample tubes. The tubes were submerged in a thermostatic water bath (Digiterm 3000542, Selecta). The color change from pale yellow brown to reddish brown indicated the reduction of silver nitrate to metallic silver. This change of color has been taken as indicative of Ag-NPs synthesis by almost all the researchers [5,17]. Once the samples were cooled down, pH of the solution was measured (pH meter Basic 20, Crison Instruments). Then, the samples were filtered through Whatman No. 1 filter paper first and centrifuged at 5000 rpm for 30 minutes. The pellet was kept in the fridge for further analysis and the maximum absorption of the supernatant was scanned at the wavelength between 200-800 nm (UV mini 1240, Shimadzu).

2.4 Characterization of Ag nanoparticles

2.4.1 UV/Vis spectroscopy

The UV/Vis spectra of the centrifugation supernatants diluted 1:10 were recorded using an UVmini-1240 spectrophotometer (Shimadzu). Different spectra were obtained showing the SPR of the prepared Ag-NPs.

2.4.2 Electron Microscopy Characterization

Field Emission Scanning Electron Microscopy (FE-SEM) coupled with an Energy-Dispersive Spectrometer (EDX) Zeiss® MERLIN FE-SEM, and a Transmission Electron Microscopy (HR-TEM) coupled to an EDX (JEM-1400 unit with an acceleration voltage of 120 kV) were used. Approximately 1 mL of sample was filtered and then dispersed in 5 mL of acetone as organic solvent and then placed in ultrasound bath for 1 h. Finally, a drop of the solution was placed on a grid and dried before TEM analysis.

The size distribution of the prepared NPs was obtained by direct observation of the TEM images and the construction of the corresponding size distribution histograms. These measurements were performed using the Image J Software, and the histograms obtained were adjusted to a 3-parameter Gaussian curve (Equation 1) where x_0 is the mean diameter (to which most nanoparticles correspond),

Peer-reviewed version available at Nanomaterials 2018, 8, 946; doi:10.3390/nano8110946

143 b is the standard deviation and a is a statistical parameter related to this fitting. Histograms were
144 calculated using the Microsoft Excel 2010, and the equation was adjusted with SigmaPlot 11.0.

$$y = ae^{\left[-0.5\left(\frac{x_0-x}{b}\right)^2\right]} \quad (1)$$

145
146 **2.4.3 Fourier Transformed Infrared (FTIR) spectroscopy**
147 To elucidate the functional groups, present in the grape stalk extract and the molecules
148 surrounding the Ag nanoparticles, FTIR spectra in the range of 4000-400 cm^{-1}, were performed in a
149 Platinum ATR spectrometer (Bruker). Both, raw extract and three times washed and centrifuged Ag-
150 NPs (to ensure the removal of unbound molecules) were freeze dried in a lyophilizer Unitop HL
151 (Virtis).
152
153 **2.4.4 Electrochemical characterization of modified SPCNFE**
154 Differential pulse anodic stripping voltammetric (DPASV) measurements were performed in an
155 Autolab System PGSTAT12 (EcoChemie, The Netherlands), in a multichannel configuration, attached
156 to a Metrohm 663 VA Stand (Metrohm, Switzerland) and a personal computer with GPES
157 Multichannel 4.7 software package (EcoChemie).
158 The auxiliary and the reference electrode (to which all potentials are referred) were Pt wire and
159 Ag|AgCl|KCl (3 mol L^{-1}) respectively, both purchased from Metrohm (Switzerland). The working
160 electrode used was a screen-printed carbon nanofiber electrode (SPCNFE) modified with silver
161 nanoparticles (Ag-NPs-SPCNFE) and connected to the Autolab Systems by means of a flexible cable
162 (ref. CAC, Dropsens). SPCNFE was a disk electrode of 4 mm diameter provided by Dropsens (ref.
163 110CNF, Oviedo, Spain).
164 Stripping voltammetric measurements using Ag-NPs-SPCNFE for the determination of Pb(II)
165 and Cd(II) ions were carried out at a deposition potential (E_d) of -1.40 V applied with stirring during
166 a deposition time (t_d) of 120 s and followed by a rest period (t_r) of 5 s. Measurements were performed
167 by scanning the potential from -1.40 to -0.30 V, and by using pulse times of 50 ms, step potentials of
168 5 mV and pulse amplitudes of 50 mV. All experiments were carried out without any oxygen removal
169 and at room temperature (20 °C).
170 Ag-NPs-SPCNFE working electrodes were prepared by drop-casting 40 µL of Ag-NPs solution
171 onto the electrode surface and drying it at 50 ºC for 30 min. The Ag-NPs solutions were
172 supernatants resulting from different washings of the pellets obtained from Ag-NPs carried out at
173 different pH values (pH 4 and 6). The corresponding pellets were suspended in 10 mL of deionized
174 water under agitation. Then the suspension was centrifuged. The resulting supernatant (W1) was
175 separated from the washed pellet. This washing operation was repeated three more times. The aim
176 of these washings was to remove non-reacted ions and molecules from the silver nanoparticles
177 suspension that could interfere on sensor response. The obtained supernatants (W1, W2, W3 and W4,
178 increasing regarding the number of times the pellets were washed) obtained from NPs synthesis,
179 were drop-casted on SPCNFE to obtain 16 different modified sensors.
180

181 **3. Results and Discussion**

182
183 **3.1 Grape stalks extracts**
184
185 To show the effect of temperature and contact time on grape stalks extraction box plots (BP) were
186 used (Figure 1). The line across the box represents the median value, whereas the top and the bottom
187 box show the location of the first and third quartiles (Q1 and Q3). The whiskers are the lines that
188 extent from the top and bottom of the box. The box itself contains the middle 50% of the data. If the
189 median is not equidistant from the top and the bottom of the box, then the data are skewed. Box

plots corresponding to total polyphenol concentration values obtained at different temperatures and at different contact times are presented in Figure 1A and 1B, respectively.

From the results of the box plots, a one-way ANOVA test was performed to analyze the differences among group means and their variation, specifically for the concentration of polyphenols and reducing sugars at different temperatures and different extraction times. The results of the ANOVA test (results not presented) showed $p < 0.05$ for the concentration of polyphenols at different temperatures and contact times and also for the concentration of reducing sugars at different contact times. However, $p > 0.05$ for the concentration of reducing sugars at different temperatures was obtained. Bonferroni post hoc test was carried out to seek out the variable responsible for significant differences between the groups of data. Results indicated that temperature is a significant variable for polyphenols concentration: p-values for the comparison between the temperatures 60 and 70ºC and 80 and 100ºC are above 0.05. Therefore, the temperature significance lies between these two groups (70-80ºC). In the case of the variable extraction time, p values were also all above 0.05 for the polyphenols and almost all below this value for the reducing sugars. These results indicate that contact time does not play a significant role in the polyphenols concentration (around 0.5 g L^{-1}) but this variable does have a significant influence in the concentration of reducing sugars (from 0.4 to 0.9 g L^{-1}).

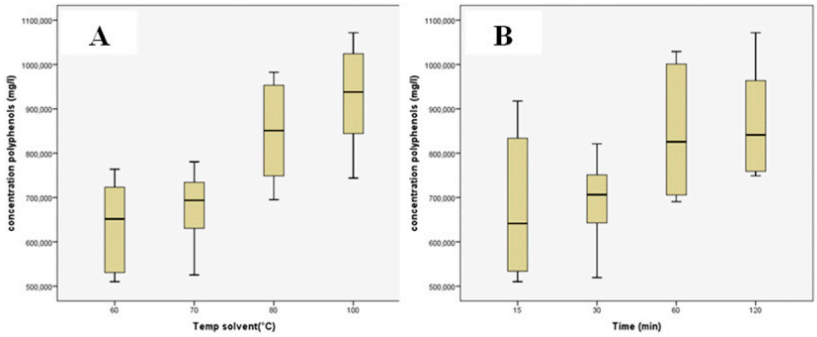

Figure 1: Boxplot for the concentration of polyphenols at different temperatures (A) and contact times (B).

3.2 Silver nanoparticles synthesis

3.2.1 FTIR characterization of grape stalk

The FTIR spectra of grape stalk (GS) extract before and after the synthesis of Ag-NPs are plotted in Figure 2. The two curves present a high variation in the intensity of bands in most of the regions of the spectrum. Dried extract spectrum displays a number of adsorption peaks indicating the complex nature of this material. The broad peak in the extract spectrum at around 3328 cm^{-1} is indicative of O-H stretching vibrations. The two peaks at 2950 and 2887 cm^{-1} correspond to the asymmetric and symmetric vibration, respectively, of C-H in the olephinic chains and the peak at 1731 cm^{-1} is attributed to the carbonyl C=O in ester groups [14]. The peaks at 1602 and 1524 cm^{-1} are due to vibration of cyclobenzene and the peaks at 1132, 1106, 1067 and 1048 can be due to C-O stretching of alcohols and phenols [22].

Preprints (www.preprints.org) | NOT PEER-REVIEWED | Posted: 22 October 2018 doi:10.20944/preprints201810.0482.v1

Peer-reviewed version available at Nanomaterials 2018, 8, 946; doi:10.3390/nano8110946

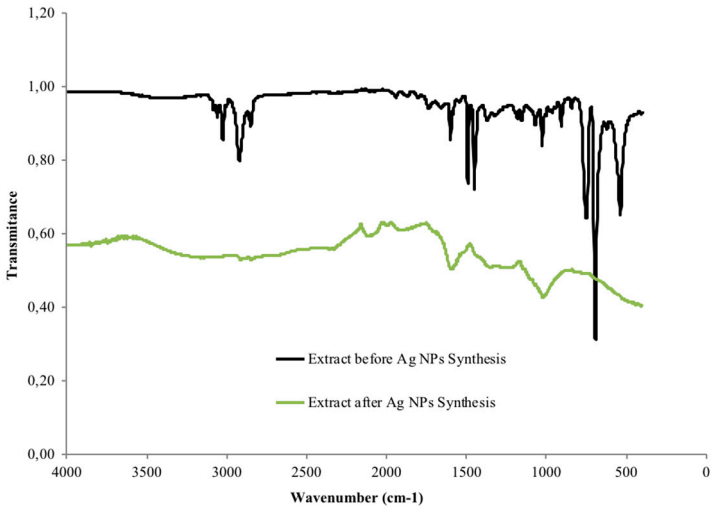

Figure 2: FTIR spectrum of dried grape stalks extract before and after the synthesis of Ag-NPs.

Dried extract spectrum after the synthesis of Ag-NPs shows a broad band in the region of OH-stretching vibrations around 3190 cm^{-1}. The shift from 3328 to 3190 cm^{-1} must be attributed to the formation of Ag-NPs. The observed broadening of the band is characteristic of hydrogen bonding (intra and inter molecular bonds). Free hydroxyl groups might interact with silver to stabilize Ag-NPs. The functional groups p-OH, m-OH and COOH of phenolic groups have been reported to act as hydrogen donor/acceptor [22, 23]. A cooperative association between phenolic compounds and other components of the extract may contribute to the stabilization of the nanoparticles [25]. The band at 1731 cm^{-1} attributed to C=O stretching mode has disappeared indicating that this group is involved in silver reduction and/or NPs stabilization. The bands corresponding to alcohol and phenol stretching shifted to lower wavenumbers and showed a very weak intensity.

3.2.2 Study of factors affecting Ag-NPs synthesis

Some physical and chemical parameters such as pH, contact time between extract and metal solution, temperature, extract/metal solution (v/v) ratio and metal salt concentration largely affect the synthesis process and the characteristics (size, shape and morphology) of the synthetized NPs [5].Therefore, the influence of these parameters on Ag-NPs synthesis mediated by grape stalk extract was investigated. Visual observation of color, changes in the pH and spectra of UV-Vis were useful tools to monitoring Ag-NPs formation.

Effect of pH

The influence of pH on Ag-NPs was investigated adjusting the pH of the extract at different pHs within 2.0-9.0, meanwhile the pH of 0.01 mol L^{-1} $AgNO_3$ solution was kept unaltered. In these experiments the volume of extract and Ag solution was 4 and 6 mL, respectively, the temperature 80ºC and the contact time 2 hours.

The nanoparticles suspension obtained from rinsing the pellet up to three times with Milli-Q water, showed maximum absorbance at around 450 nm, indicating the presence of Ag nanoparticles. It has been reported that silver colloids exhibit maximum absorbance within the range 400-500 nm due to Surface Plasmon Resonance (SPR) [26–28].

As can be seen in Figure 3A, a peak at 307 nm was observed. This peak must be attributed to the organic matter of the GS extract. This peak is very high in the solution at pH 2, when any other peak was clearly observed. In case of pH 4 and 6, a peak around 450 nm was observed. This peak can be attributed to the SPR of silver nanoparticles as mentioned in section 2.3.1. It must be remarked that the absorbance of peak from solution at pH 6 was higher than that at pH 4. As peak intensity could be related to Ag-NPs concentration, the increase on peak intensity of solution at pH 6 compared to pH 4 could indicate higher nanoparticles presence in solution. Two peaks were observed in the UV-Vis plot of pH 8 solution and both peaks are in the Ag-NP SPR range. The wavelength of the band

Peer-reviewed version available at Nanomaterials 2018, 8, 946; doi:10.3390/nano8110946

shifted to 470 nm when the reaction pH was 4 and 6. The shift towards large wavelengths (red shift) indicates an increase in the mean diameter of Ag-NPs [25, 26].
The high band observed at 440 nm seems indicate a great number of Ag-NPs. Additionally, the shift towards lower wavelengths indicates a decrease in the mean diameter of Ag NPs [25, 26]. Thus, SPR seems indicate a great number of smaller diameter Ag-NPs when synthesis takes place at pH 8. Nevertheless, the additional peak observed at 415 nm indicates the presence of other compounds in solution that could affect Ag-NPs quality.

Effect of contact time

In order to ascertain the time required for the completion of the reduction reaction, several tubes containing 4 mL of extract and 6 mL of 0.01 mol L^{-1} $AgNO_3$ were heated at 80°C. The tubes were removed from the thermostatic bath at different times ranging from 5 min to 8 h.
The UV-Vis spectra of Ag-NPs solution obtained at different reaction times are depicted in Figure 3B. In the experimental conditions used (4 mL extract, 6 mL 0.01 M $AgNO_3$, 80°C, pH 4) the Ag-NPs SPR band is noticeable after 5 min of reaction. Up to this reaction time the absorbance intensity increased with time, suggesting a great number of nanoparticles in the solution.
The pH of the reaction mixture was measured before and after the reduction reaction. The initial pH (4.01) increased in the first 5 min to 4.15 and then progressively diminished with time and reached the pH value 3.02 after 8h. The change of pH might be related to the involvement of some compounds in the reduction or capping processes leading to Ag-NPs formation.

Effect of extract/silver solution (v/v) ratio

Different volume of extract and silver solution ratios were investigated in order to determine the effect of silver addition and the effect of extract addition, respectively. The first one consisted in fixing the volume of extract (4 mL) and adding different volumes (1-6 mL) of 0.01 mol L^{-1} $AgNO_3$. In the second one the volume of silver solution was fixed (1 mL) and the volume of extract was varied (1-9 mL). For both sets of experiments total volume in the tubes was adjusted to 10 mL by adding Milli-Q water. Heating temperature of 80°C and contact time of 2 hours were kept as when studying effect of pH.
The plot of the spectra obtained at increasing volumes of extract is presented in Figure 3C. The reacted solutions exhibited an intense dark reddish-brown color with independence of the volume of extract added to 1 mL 0.01 mol L^{-1} $AgNO_3$. The increasing sharp peak at 307 nm refers to light absorption of extract components at this wavelength. As expected, absorbance intensity at this wavelength increases with the addition of more volume of extract. Maximum absorbance intensity of the SPR band increased with the addition of 1 to 5 mL of extract. Higher volumes of extract led to the opposite trend as absorbance values decreased with the extra extract addition. The decrease of absorbance could be due to the deficiency of silver ions with respect to the amount of biomolecules that could provoke the agglomeration of smaller particles to form larger Ag-NPs that would absorb light in a lower extent [29]. SPR band values shifted from 447.5 to 459 nm with the addition of extract volume from 1 to 9 mL, indicating the effect of extract concentration in the mean diameter of Ag-NPs. López-Carrillo *et al*. [31], reported that in general, particle size can be controlled by changing the volume of the reducing agent.

Peer-reviewed version available at Nanomaterials 2018, 8, 946; doi:10.3390/nano8110946

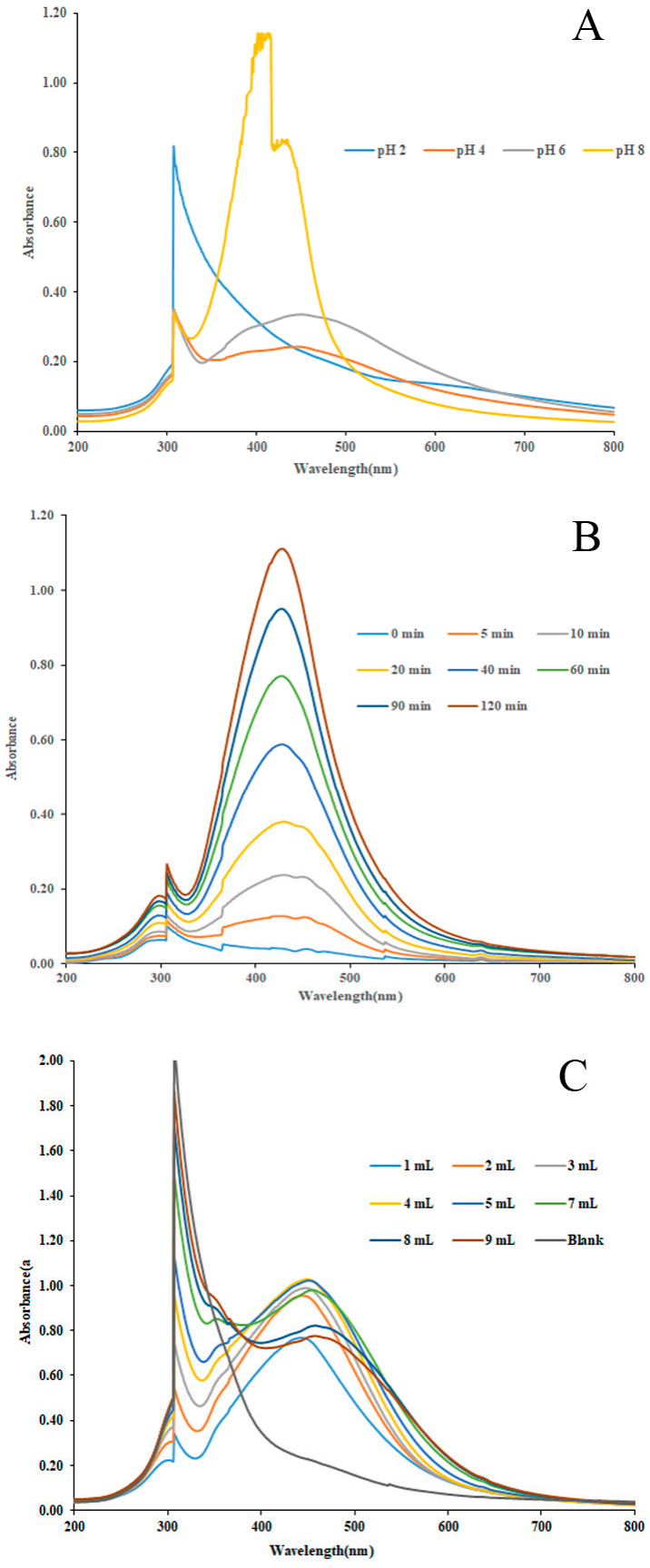

Figure 3: UV/Vis Spectra showing the influence of different parameters in the synthesis of Ag-NPs with the GS extract: A) pH, B) contact time and C) extract addition.

3.2.5 Electron Microscopy Characterization

The suitability of the GS extract for the synthesis of Ag-NPs was proved by direct observation of SEM and TEM images. As an example, Figure 4 shows the electron microscopy characterization for a sample solution of NPs synthetized at pH 4. Results reveal that Ag-NPs are obtained through this methodology with an average diameter of (27.7 ± 0.6) nm. Moreover, the chemical identity of the Ag-NPs is proved by EDX spectra presented as well in Figure 4 (B, D).

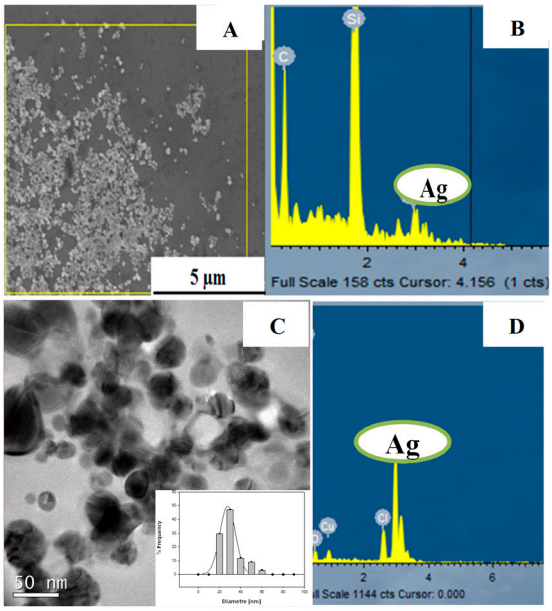

Figure 4: Electron Microscopy micrographs for Ag-NPs synthesized at pH 4 using the GS extract as reducing agent. SEM micrograph (A) and corresponding EDX spectra (B) and TEM micrograph (C) with size distribution histogram inset with the corresponding EDX spectra (D).

The size distribution analysis for the different Ag-NPs synthetized at different pH and measured by TEM images was determined and it is summarized in Table I. Due to the higher surface to volume ratio, these Ag-NPs can present higher electrocatalytical activity, and therefore they could be suitable for the modification of electrodes, as well be addressed in the following section.

Table I: Diameter measurements from TEM micrographs as for Ag-NPs prepared at different pH

Sample preparation pH	Diameter (nm)
2	55.4 ± 0.3
4	27.7 ± 0.6
6	54.3 ± 0.1
8	9.0 ± 0.2

As can be seen, the smaller particles size of Ag-NPs was obtained when synthesis was carried out at pH 8, confirming the result of the effect of pH on Ag-NPs synthesis analyzed by UV-VIS spectra. Similar nanoparticle diameters were obtained when synthesis was carried out at pH 2 and pH 6. Thus, TEM results confirm the effect of pH on nanoparticle size. Nevertheless, other aspects related to size stabilization seem to influence in great extent on size particle than pH, as no clear trend between pH and size was observed.

Figure 5 presents SEM images of a the non-modified(5A) and Ag NPs-modified(5B and 5C) SPCNFEs, showing that the drop-casting strategy does not alter the morphology of the electrode, but leads to the incorporation of the green synthesized Ag NPs, distribute all over the surface(5C). This fact is relevant for the enhancement of the electroanalytical features of the SPCNFE.

Peer-reviewed version available at Nanomaterials 2018, 8, 946; doi:10.3390/nano8110946

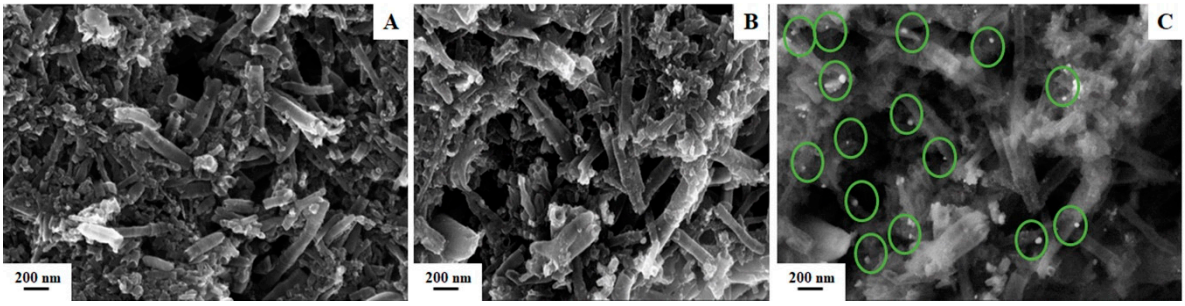

Figure 5: SEM InLens images of raw SPCNFE (A) and SPCNFE after the drop casting of Ag-NPs (B). SEM Secondary Lens of SPCNFE highlighting the location of the drop-casted Ag-NPs.

3.2.6 Electrochemical Characterization

The selected E_d, t_d and t_r were firstly optimized to ensure the simultaneous determination of Cd(II) and Pb(II) at each Ag-NPs-SPCNFE in the selected concentration range (data not shown), being for all cases a E_d of -1.40 V applied with stirring during a t_d of 120 s and followed by a t_r of 5 s.

The comparison of the analytical performance of the SPCNFE modified with Ag-nanoparticles obtained from different synthesis pH and after two or three additional rinsing suspensions (W3 and W4) is shown in Figure 6. In order to study the effect of the NP size on the electrochemical behavior and to avoid the presence of other compounds in solution, Ag-NPs obtained at pH 4 and 6 were chosen to prepare SPCNFE. The aim of the modified Ag-NPs-SPCNFE is the simultaneous determination of a solution containing Pb(II) and Cd(II). Well-defined peaks can be observed for both Pb(II) and Cd(II) ions at -0.42 and -0.55 V, respectively, with all electrodes. However, more intense peaks are obtained using the SPCNFE modified with Ag-NPs prepared at pH 4, supernatant W3 (SPCNFE – pH4.W3), particularly in the case of Cd(II).

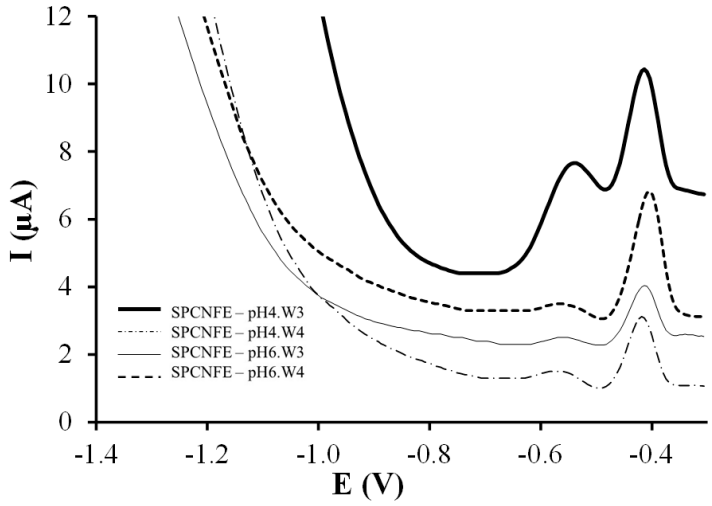

Figure 6: Stripping voltammetric measurements of the SPCNFE modified with Ag-NPs obtained from different synthesis pH conditions and washing suspensions for the simultaneous detection of Cd(II) and Pb(II) at 77 µg L^{-1} and pH 4.5

Simultaneous calibration of Pb(II) and Cd(II) ions by DPASV were carried out on each Ag- NPs-SPCNFE. For this purpose, 9 increasing concentrations of Pb(II) and Cd(II) ranging from 1.1 to 100.4 and from 1.1 to 100.1 µg L^{-1}, respectively, were used as calibration samples. Figure 7 shows, as an example, the evolution of the DPASV signals of both metal ions using SPCNFE modified with silver nanoparticles obtained from SPCNFE–pH4.W3 when their concentrations increase (the other three Ag-NPs-SPCNFE present equivalent behaviors). The obtained calibration data on each Ag-NPs-SPCNFE are summarized in Table II. The limit of detection (LOD) was calculated as 3 times the standard deviation of the intercept over the slope of the calibration curve of the target ions. The limit

Peer-reviewed version available at Nanomaterials 2018, 8, 946; doi:10.3390/nano8110946

of quantification (LOQ) was evaluated by considering 10 times the previous ratio. The lowest value of the linear concentration range was established from the corresponding LOQ. As shown in Table II, linear calibration curves were obtained for Pb(II) and Cd(II) up to a maximum concentration level of 100.4 and 27.5-39.7 μg L^{-1}, respectively, depending on the considered Ag-NPs-SPCNFE. Regarding sensitivities (nA μg^{-1} L), obtained from the slope of the calibration curves, they varied from 21.2 to 62 for Pb(II) and from 5.1 to 46 for Cd(II) depending on the Ag-NPs-SPCNFE (Table II). The LOD of the determination of the two metals in the four considered Ag-NPs-SPCNFEs ranged from 2.7 to 4.9 for Pb(II) and from 2.8 to 8.1 for Cd(II) according to the considered Ag-NPs-SPCNFE, whereas the LOQ varied from 8.9 to 16.2 for Pb(II) and from 9.5 to 26.9 for Cd(II) (as seen in Table II). It should be mentioned that no previous LOD and LOQ data for SPCNFEs modified with Ag-NPs from natural sources are available in the literature. Nevertheless, as compared to previous results reported using other electrodes, e. g., synthetic Ag-NPs based electrodes [16,32], bismuth film electrodes [33], antimony film electrodes [33], chemically modified electrodes [34–37], the LOD and LOQ achieved in this work for Cd(II) and Pb(II) are similar or even lower depending on the considered modified electrode.

Therefore, the reported calibration data suggests that all the considered Ag-NPs-SPCNFEs could be suitable and a valuable option to more conventional electrodes for the simultaneous determination of Pb(II) and Cd(II) at trace levels in natural samples. However, the best results (higher sensitivities, lower LODs and wider linear ranges) were obtained with SPCNFE-pH4.W3

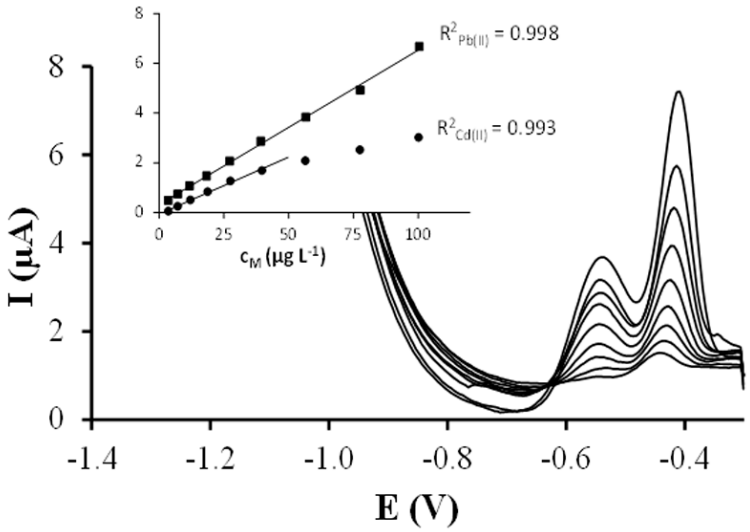

Figure 7: DPASV measurements and calibration curves (insets) obtained for the simultaneous calibration of Pb(II) and Cd(II) in acetate buffer pH 4.5 using an Ag-NPs modified -SPCNFE at an E_d of -1.4 V and a t_d of 120 s.

Peer-reviewed version available at Nanomaterials 2018, 8, 946; doi:10.3390/nano8110946

Sample	Pb(II)	Cd(II)
SPCNFE – pH4.W3		
Sensitivity (nA μg^{-1} L)	62 (1)	46 (2)
R^2	0.998	0.993
Linear range[a] ($\mu g\ L^{-1}$)	8.9-100.4	9.5-39.7
LOD ($\mu g\ L^{-1}$)	2.7	2.8
SPCNFE – pH4.W4		
Sensitivity (nA μg^{-1} L)	26.0 (0.7)	8.5 (0.5)
R^2	0.996	0.993
Linear range[a] ($\mu g\ L^{-1}$)	13.3-100.4	16.0-39.7
LOD ($\mu g\ L^{-1}$)	4.0	4.8
SPCNFE – pH6.W3		
Sensitivity (nA μg^{-1} L)	21.2 (0.5)	5.1 (0.5)
R^2	0.996	0.980
Linear range[a] ($\mu g\ L^{-1}$)	12.3-100.4	26.9-39.7
LOD ($\mu g\ L^{-1}$)	3.7	8.1
SPCNFE – pH6.W4		
Sensitivity (nA μg^{-1} L)	43 (1)	13.8 (0.8)
R^2	0.993	0.989
Linear range[a] ($\mu g\ L^{-1}$)	16.2-100.4	10.0-27.5
LOD ($\mu g\ L^{-1}$)	4.9	3.0

Table II. Calibration data for the simultaneous determination of Pb(II) and Cd(II) at each Ag-NPs-SPCNFE at E_d of -1.4 V, t_d of 120 s and pH 4.5. Standard deviations are denoted by parenthesis.

4. Conclusions

An environmentally friendly preparation of Ag-NPs by using non-toxic reduction chemicals has been developed. Thus, total polyphenols and reducing sugars present in plant extracts from grape stalk wastes were used as reducing agents and stabilizers in the nanoparticles production. The extract and the Ag-NPs generation have been studied and optimized considering several parameters and have been fully characterized by different spectroscopic and electron microscopy techniques. Finally, these Ag-NPs were drop-casted on the SPCNFE and the resulting sensors were analytically characterized in order to proof their suitability for sensing purposes. These modified Ag-NPs-SPCNFE were tested

for the simultaneous voltammetric stripping determinations of Pb(II) and Cd(II) providing good reproducibility, sensitivity, lineal range and limits of detection at μg L^{-1} range; more precisely $LOD_{Pb(II)}$ 2.7 μg L^{-1} and $LOD_{Cd(II)}$ 2.8 μg L^{-1}, evidencing the enhancement of the SPCNFE electrodes by adding the above mentioned Ag-NPs.

Author Contributions: Julio Bastos-Arrieta and Antonio Florido carried out the analysis data obtained from the synthesis and microscopic characterization of silver nanoparticles. Clara Pérez-Ràfols and Núria Serrano carried out the modification of screen-printed electrodes with nanoparticles, the voltammetric measurements and the data treatment. Núria Fiol, Jordi Poch and Isabel Villaescusa carried out the preparation and characterization of the grape stalk, besides the green synthesis of the Ag NPs. All authors contributed to the writing, revision and critical discussion of the results presented in the final version of the manuscript.

Funding: This research has been supported by Ministerio de Economia y Competitividad (MINECO) and Fondo Europeo de Desarrollo Regional (FEDER), projects CTM2015-68859-C2-1-R and C2-2-R, and by the Generalitat de Catalunya (Projects 2017SGR311 and 2017SGR312).

Acknowledgments: Clara Pérez-Ràfols also acknowledges the Ministerio de Educación, Cultura y Deporte (MECD) for a Ph.D. grant. Special thanks to Nathalie Gerits, Jeongeun Kim and Pau-Isai Jaile for helping in part of the experimental work

Conflicts of Interest: The authors declare no conflict of interest

References

1. Zhang, X.; Yan, S.; Tyagi, R. D.; Surampalli, R. Y. Synthesis of nanoparticles by microorganisms and their application in enhancing microbiological reaction rates. *Chemosphere* **2011**, *82*, 489–494, doi:10.1016/j.chemosphere.2010.10.023.
2. Sharma, D.; Kanchi, S.; Bisetty, K. Biogenic synthesis of nanoparticles: A review. *Arab. J. Chem.* **2015**, doi:10.1016/j.arabjc.2015.11.002.
3. Kuppusamy, P.; Yusoff, M. M.; Maniam, G. P.; Govindan, N. Biosynthesis of metallic nanoparticles using plant derivatives and their new avenues in pharmacological applications – An updated report. *Saudi Pharm. J.* **2016**, *24*, 473–484, doi:10.1016/j.jsps.2014.11.013.
4. Mittal, A. K.; Chisti, Y.; Banerjee, U. C. Synthesis of metallic nanoparticles using plant extracts. *Biotechnol. Adv.* **2013**, *31*, 346–356, doi:10.1016/j.biotechadv.2013.01.003.
5. Srikar, S. K.; Giri, D. D.; Pal, D. B.; Mishra, P. K.; Upadhyay, S. N. Green Synthesis of Silver Nanoparticles: A Review. *Green Sustain. Chem.* **2016**, *06*, 34–56, doi:10.4236/gsc.2016.61004.
6. He, Y.; Du, Z.; Lv, H.; Jia, Q.; Tang, Z.; Zheng, X.; Zhang, K.; Zhao, F. Green synthesis of silver nanoparticles by Chrysanthemum morifolium Ramat. extract and their application in clinical ultrasound gel. *Int. J. Nanomedicine* **2013**, *8*, 1809–1815, doi:10.2147/IJN.S43289.
7. Ravichandran, V.; Vasanthi, S.; Shalini, S.; Ali Shah, S. A.; Harish, R. Green synthesis of silver nanoparticles using Atrocarpus altilis leaf extract and the study of their antimicrobial and antioxidant activity. *Mater. Lett.* **2016**, *180*, 264–267, doi:10.1016/j.matlet.2016.05.172.
8. Ahmed, S.; Ahmad, M.; Swami, B. L.; Ikram, S. A review on plants extract mediated synthesis of silver nanoparticles for antimicrobial applications: A green expertise. *J. Adv. Res.* **2016**, *7*, 17–28, doi:10.1016/J.JARE.2015.02.007.
9. Kuppusamy, P.; Ichwan, S. J. A.; Parine, N. R.; Yusoff, M. M.; Maniam, G. P.; Govindan, N. Intracellular biosynthesis of Au and Ag nanoparticles using ethanolic extract of Brassica oleracea L. and studies on their physicochemical and biological properties. *J. Environ. Sci. (China)* **2015**, *29*, 151–157, doi:10.1016/j.jes.2014.06.050.
10. Luo, F.; Yang, D.; Chen, Z.; Megharaj, M.; Naidu, R. Characterization of bimetallic Fe/Pd nanoparticles by grape leaf aqueous extract and identification of active biomolecules involved in the synthesis. *Sci.*

Total Environ. **2016**, *562*, 526–532.

11. Venkateswarlu, S.; Natesh Kumar, B.; Prathima, B.; Anitha, K.; Jyothi, N. V. V A novel green synthesis of Fe3O4-Ag core shell recyclable nanoparticles using Vitis vinifera stem extract and its enhanced antibacterial performance. *Phys. B Condens. Matter* **2015**, *457*, 30–35, doi:10.1016/j.physb.2014.09.007.
12. Dziwoń, K.; Pulit-Prociak, J.; Banach, M. Green technologies in obtaining nanomaterials–using white grapes (Vitis vinifera) in the processes for the preparation of silver nanoparticles. **2015**.
13. Krishnaswamy, K.; Vali, H.; Orsat, V. Value-adding to grape waste: Green synthesis of gold nanoparticles. *J. Food Eng.* **2014**, *142*, 210–220, doi:10.1016/j.jfoodeng.2014.06.014.
14. Pujol, D.; Liu, C.; Fiol, N.; Olivella, M. À.; Gominho, J.; Villaescusa, I.; Pereira, H. Chemical characterization of different granulometric fractions of grape stalks waste. *Ind. Crops Prod.* **2013**, *50*, 494–500.
15. Muñoz, J.; Bastos-Arrieta, J.; Munoz, M.; Muraviev, D. N.; Céspedes, F.; Baeza, M. Simple green routes for the customized preparation of sensitive carbon nanotubes/epoxy nanocomposite electrodes with Functional Metal Nanoparticles. *RSC Adv.* **2014**, *4*, 44517–44524, doi:10.1039/C4RA07294D.
16. Pérez-Ràfols, C.; Bastos-Arrieta, J.; Serrano, N.; Díaz-Cruz, J. M.; Ariño, C.; de Pablo, J.; Esteban, M. Ag nanoparticles drop-casting modification of screen-printed electrodes for the simultaneous voltammetric determination of Cu(II) and Pb(II). *Sensors (Switzerland)* **2017**, *17*, doi:10.3390/s17061458.
17. Lu, Y.; Liang, X.; Niyungeko, C.; Zhou, J.; Xu, J.; Tian, G. A review of the identification and detection of heavy metal ions in the environment by voltammetry. *Talanta* **2018**, *178*, 324–338.
18. Economou, A. Screen-printed electrodes modified with "green" metals for electrochemical stripping analysis of toxic elements. *Sensors (Switzerland)* 2018, *18*, 1032.
19. Pérez-Ràfols, C.; Serrano, N.; Díaz-cruz, J. M.; Ariño, C.; Esteban, M. New approaches to antimony film screen-printed electrodes using carbon-based nanomaterials substrates. *Anal. Chim. Acta* **2016**, *916*, 17–23, doi:10.1016/j.aca.2016.03.003.
20. Arthur Israel, V. Vogel's textbook of quantitative chemical analysis. In; Longman Scientific & Technical, 1989.
21. Ramteke, C.; Chakrabarti, T.; Sarangi, B. K.; Pandey, R. Synthesis of Silver Nanoparticles from the Aqueous Extract of Leaves of Ocimum sanctum for Enhanced Antibacterial Activity. *Hindawi Publ. Corp. J. Chem.* **2013**, *2013*, 1–8, doi:10.1155/2013/278925.
22. Xu, H.; Wang, L.; Su, H.; Gu, L.; Han, T.; Meng, F.; Liu, C. Making good use of food wastes: green synthesis of highly stabilized silver nanoparticles from grape seed extract and their antimicrobial activity. *Food Biophys.* **2015**, *10*, 12–18.
23. Tchaikovskaya, O. N.; Basyl', O. K.; Sultimova, N. B. Proton-acceptor and proton-donor properties of phenol and its substitutes. *Russ. Phys. J.* **2005**, *48*, 1245–1250, doi:10.1007/s11182-006-0054-4.
24. Lerma-garcía, M.; Ávila, M.; Simó-alfonso, E. F.; Ríos, Á.; Zougagh, M. Synthesis of gold nanoparticles using phenolic acids and its application in catalysis. **2014**, *5*, 1919–1926.
25. Mehanna, N. S.; Hassan, Z. M. R.; El-Din, H. M. F.; Ali, A. A.-E.; Amarowicz, R.; El-Messery, T. M. Effect of Interaction Phenolic Compounds with Milk Proteins on Cell Line. *Food Nutr. Sci.* **2014**, *5*, 2130–2146.
26. Fran ccedil ois, E. rsquo ane M.; Marcelle, L. S.; Cecile, O. E.; Agnes, A. N.; Djiopang, Y. S.; Fanny, A. E. M.; Lidwine, N.; Harouna, M.; Emmanuel, M. M. Unexplored vegetal green synthesis of silver nanoparticles: A preliminary study with Corchorus olitorus Linn and Ipomea batatas (L.) Lam. *African J. Biotechnol.* **2016**, *15*, 341–349, doi:10.5897/AJB2015.14962.
27. Demirbas, A.; Welt, B. A.; Ocsoy, I. Biosynthesis of red cabbage extract directed Ag NPs and their effect

on the loss of antioxidant activity. *Mater. Lett.* **2016**, *179*, 20–23, doi:10.1016/j.matlet.2016.05.056.

28. Velgosová, O.; Mražíková, A.; Marcinčáková, R. Influence of pH on green synthesis of Ag nanoparticles. *Mater. Lett.* **2016**, *180*, 336–339, doi:10.1016/j.matlet.2016.04.045.
29. Ajitha, B.; Kumar Reddy, Y. A.; Reddy, P. S.; Jeon, H.-J.; Ahn, C. W. Role of capping agents in controlling silver nanoparticles size, antibacterial activity and potential application as optical hydrogen peroxide sensor. *RSC Adv.* **2016**, doi:10.1039/C6RA03766F.
30. Khalil, M. M. H.; Ismail, E. H.; El-Baghdady, K. Z.; Mohamed, D. Green synthesis of silver nanoparticles using olive leaf extract and its antibacterial activity. *Arab. J. Chem.* **2014**, *7*, 1131–1139, doi:10.1016/j.arabjc.2013.04.007.
31. Carrillo-Lï¿½pez, L. M.; Morgado-Gonzï¿½lez, A.; Morgado-Gonzï¿½lez, A. Biosynthesized Silver Nanoparticles Used in Preservative Solutions for Chrysanthemum cv. Puma. *J. Nanomater.* **2016**, *2016*, doi:10.1155/2016/1769250.
32. Prakash, S.; Shahi, V. K. Analytical Methods. **2011**, 2134–2139, doi:10.1039/c1ay05265a.
33. Serrano, N.; Alberich, A.; Díaz-Cruz, J. M.; Ariño, C.; Esteban, M. Coating methods, modifiers and applications of bismuth screen-printed electrodes. *TrAC - Trends Anal. Chem.* **2013**, *46*, 15–29, doi:10.1016/j.trac.2013.01.012.
34. Pérez-Ràfols, C.; Serrano, N.; Díaz-Cruz, J. M.; Ariño, C.; Esteban, M. Glutathione modified screen-printed carbon nanofiber electrode for the voltammetric determination of metal ions in natural samples. *Talanta* **2016**, *155*, 8–13, doi:10.1016/j.talanta.2016.04.011.
35. Pérez-Ràfols, C.; Serrano, N.; Díaz-Cruz, J. M.; Ariño, C.; Esteban, M. Penicillamine-modified sensor for the voltammetric determination of Cd (II) and Pb (II) ions in natural samples. *Talanta* **2015**, *144*, 569–573.
36. Serrano, N.; González-Calabuig, A.; del Valle, M. Crown ether-modified electrodes for the simultaneous stripping voltammetric determination of Cd (II), Pb (II) and Cu (II). *Talanta* **2015**, *138*, 130–137.
37. Serrano, N.; Prieto-Simón, B.; Ceto, X.; del Valle, M. Array of peptide-modified electrodes for the simultaneous determination of Pb (II), Cd (II) and Zn (II). *Talanta* **2014**, *125*, 159–166.